77-88

BUCKLING OF CYLINDERS IN A CONFINING MEDIUM

C. V. Chelapati, California State College at Long Beach; and
J. R. Allgood, U. S. Naval Civil Engineering Laboratory,
Port Hueneme, California

A large-deflection theory is presented for defining the critical radial pressures that result in the buckling of elastically supported homogeneous cylinders with simple ends. Solutions are given for radial support around the extrados and for radial support only on the outward acting lobes of the circumferential waves that form on loading. It is shown that the difference between the energy load and the Euler load is a maximum for cylinders with no radial support and that the energy load approaches the Euler load as the length-to-radius ratio and the foundation coefficient decrease and as the radius-to-thickness ratio increases. Critical pressures are greater for cylinders supported around the entire extrados than for cylinders supported only on the outward displacing lobes. Practical utility of the theory is found in its application to conduits and cylindrical protective structures buried in soil fields. For such applications, the equation defining the lower bound of buckling is modified to permit one to account for the influence of the surface boundary and to include soil parameters that are readily obtainable in the laboratory. A few tests were performed to check the theory. The results of these tests and other available data agree reasonably well with the theory.

•SOLUTIONS to the problem of defining the strength of conduits, tunnel liners, and cylindrical shelters buried in soil depend on the ability of engineers to predict buckling loads. The general purpose of this paper is to provide the needed solutions. Specific objectives were to define and compare the Euler and energy loads, study the effect of all-around support as compared to support only on outward-deflecting lobes, determine the influence of the dominant parameter on buckling resistance, and compare the results of the elastic theory solutions with experimental results. These goals were pursued to provide improved criteria and methods for the design of buried cylinders.

The configuration analyzed (Fig. 1) consists of a radially supported cylinder with a bonded interface and simple ends. The cylinder is subjected to uniform radial pressure. Two types of radial support are considered: elastic support around the complete perimeter and elastic support only on the outward-deflecting portions of the lobes that form during loading. Parallel solutions are developed from the theory for both of these cases.

In studying the buckling of shells, von Karman and Tsein (1) showed that some systems have states of stable equilibrium at loads less than the Euler load. These states of equilibrium are separated by "energy barriers" such that work must be expended to pass from the unbuckled to the buckled configuration. Such work might be supplied by perturbations in the load or by other means; consequently, the critical load may be less than the Euler load as shown in Figure 2.

Subsequent to the work of von Karman and Tsein, Friedrichs (2) pointed out that at state B′ (Fig. 2) the potential energy, V, is greater than at B; consequently, buckling is not likely at a load less than p_n where the potential energy in the two states is equal. The latter condition is indicated qualitatively by points D and D′ (Fig. 2). The load p_n will be referred to as the transitional buckling load or the energy load.

Sponsored by Committee on Subsurface Soil-Structure Interaction.

A number of investigators, the earliest of whom was Link (3), have developed plane strain solutions for elastically supported cylinders by using the classical small-deformation theory. Later, Luscher endeavored to fit such relations to data from tests of buried cylinders (4).

Langhaar and Boresi (5) derived an expression for the energy load for cylinders subjected to hydrostatic loading and found that the energy to cause a transition from the unbuckled to the buckled state is small and could easily be supplied by accidental shocks. Their work was subsequently compared with the results of experiments by Kirstein and Wenk (6) who observed both elastic snap-through and recovery.

Forrestal and Herrmann (7) showed that the Poisson's ratio of a confining medium has less than a 15 percent effect on the critical load but that the presence or absence of interface shear has a relatively large effect for confining media with low Poisson's ratios.

In studies of other geometries, Gjelsvik and Bodner (8) found that the energy load is relatively insensitive to the assumption (number of terms in the series) for the deflected shape.

In the following sections, the Euler and energy loads are investigated by modifying the methodology of Langhaar and Boresi to include terms that contain the strain energy of the support. The solutions are compared with the results of experiments on cylinders buried in sand.

DEVELOPMENT OF BUCKLING EQUATIONS

The general procedure for the theoretical development is to express the strain energy and the potential energy in terms of displacement by using the large-deflection theory. Then the various energy components are summed to obtain the increment of total potential energy, which is set to zero to obtain the critical pressures.

FORMULATION OF DISPLACEMENT RELATIONS

Rectangular and cylindrical coordinates for a cylinder are shown in Figure 1b, where the origin of coordinates is taken at the center of the section at midlength. Let u, v, and w represent the axial, circumferential, and radial displacements respectively of the point P due to buckling. The components of strain may be expressed in terms of these displacement components and the coordinates as (5)

$$\left.\begin{aligned} \epsilon_x &= \epsilon_x^{(o)} + u_x + \tfrac{1}{2} v_x^2 + \tfrac{1}{2} w_x^2 \\ \epsilon_\theta &= \epsilon_\theta^{(o)} + [(v_\theta + w)/a] + \tfrac{1}{2} [(v - w_\theta)/a]^2 \\ \gamma_{x\theta} &= (u_\theta/a) + (v_x - w_x)[(v - w_\theta)/a] \end{aligned}\right\} \quad (1)$$

In these expressions, the subscripts on displacements denote partial derivatives, ϵ_x is the axial strain, ϵ_θ is the circumferential strain, and $\gamma_{x\theta}$ is the shearing strain. The strains at incipient buckling are denoted by $\epsilon_x^{(o)}$ and $\epsilon_\theta^{(o)}$.

Because u, v, and w are unknown, the shape after buckling has to be assumed so that we can compute the changes in total potential energy. They are assumed to be represented by the terms containing up to $3n\theta$ of the Fourier series as

$$\left.\begin{aligned} u &= u_0 + u_1 \cos n\theta\ u_2 \cos 2n\theta + u_3 \cos 3n\theta \\ v &= v_1 \sin n\theta + v_2 \sin 2n\theta + v_3 \sin 3n\theta \\ w &= w_0 + w_1 \cos n\theta + w_2 \cos 2n\theta + w_3 \cos 3n\theta \end{aligned}\right\} \quad (2)$$

where u_i, v_i, and w_i are functions of x alone and n denotes the number of complete waves around the perimeter.

If we also assume that the incremental circumferential strain, $\Delta\epsilon_\theta$, is equal to zero, Eq. 1 yields

$$\Delta\epsilon_\theta = \epsilon_\theta - \epsilon_\theta^{(o)} = [(v_\theta + w)/a] + \tfrac{1}{2}[(v - w_\theta)/a]^2 = 0 \tag{3}$$

By substituting the expressions for v and w in Eq. 2 in Eq. 3 and by regrouping terms, we can show that all the coefficients v_i and w_i can be expressed in terms of w_1 alone as follows:

$$\left.\begin{aligned} v_1 &= -(w_1/n) \\ v_2 &= n[n - (1/n)]^2 w_1^2/[2a(4n^2 - 1)] \\ v_3 &= 0 \end{aligned}\right\} \tag{4}$$

$$\left.\begin{aligned} w_0 &= -\{[n - (1/n)]^2 w_1^2\}/4a \\ w_1 &= w_1 \\ w_2 &= -\{[n - (1/n)]^2 w_1^2\}/[4a(4n^2 - 1)] \\ w_3 &= 0 \end{aligned}\right\} \tag{5}$$

On the basis of experimental data, it is assumed that

$$w_1/a = [W_o \cos(\pi x/L)]/[n - (1/n)] \tag{6}$$

where W_o is a constant, n is the number of circumferential waves around the perimeter, and L is the length of the cylinder. These displacement relations permit one to express the components of the total potential energy in terms of W_o^2 as exemplified in the following section.

Strain Energy Due to Radial Support

All-Around Support—The change in strain energy due to radial support is given by

$$\Delta U_s = 2a \int_0^{\frac{L}{2}} \int_0^{2\pi} (k_z w^2/2)\, d\theta dx \tag{7}$$

where k_z is the coefficient of soil reaction in lb/in.^{2}/in. or other consistent units.

Substitution of Eqs. 2 and 6 in Eq. 7, integration, and elimination of dimensions by EahL give

$$\Delta U_s/EahL = k_z a/[E(h/a)^3](h/a)^2 (d_1 W_o^2 + d_2 W_o^4) \tag{8}$$

where

$d_1 = \pi n^2/[4(n^2 - 1)^2]$, and
$d_2 = [3\pi(32n^4 - 16n^2 + 3)]/[256(4n^2 - 1)^2]$

Outward Lobe Support—In deriving Eq. 8, it was assumed that the radial support is effective for both positive and negative values of the displacement w, the positive direction of w indicating the outward radial displacement.

With radial support only for positive values of the radial displacement, strain energy is stored in regions of positive displacement, w, and is zero for portions with negative displacement. It is assumed that the strain energy stored in the media is equal to the strain energies because the components of the displacement w are imposed separately. Thus, recognizing that w_3 is zero by using Eq. 5, we may write the strain energy as

$$\Delta\overline{U}_s = k_z a^3 \int_0^{\frac{L}{2}} \left\{ \int_0^{2\pi} (w_0/a)^2 \, d\theta + n \int_0^{\frac{2\pi}{2n}} [(w_1/a)\cos n\theta]^2 \, d\theta \right.$$

$$\left. + 2n \int_{\frac{2\pi}{8n}}^{\frac{6\pi}{8n}} [(w_2/a) \cos 2n\theta]^2 \, d\theta \right\} dx \qquad (9)$$

The first term does not contribute to $\Delta\overline{U}_s$ because w_0 is negative; therefore,

$$\Delta\overline{U}_s = k_z a^3 \int_0^{\frac{L}{2}} [(w_1/a)^2 (\pi/2) + (w_2/a)^2 (\pi/2)] \, dx \qquad (10)$$

If we use Eqs. 4 and 6 (eliminating dimensions by EahL) and simplify, the change in strain energy is

$$\Delta\overline{U}_s/EahL = k_z a/[E(h/a)^3] (h/a)^2 (\overline{d}_1 W_o^2 + \overline{d}_2 W_o^4) \qquad (11)$$

where

$\overline{d}_1 = \pi n^2/[8(n^2 - 1)^2]$, and
$\overline{d}_2 = 3\pi/[512(4n^2 - 1)^2]$.

Other Components of Total Potential Energy

Expressions for the strain energy components, ΔU, due to membrane stresses and bending stresses and the increment of potential energy, $\Delta\Omega_p$, due to external pressure (as developed by Langhaar and Boresi, 5) are given below. ΔU due to membrane stresses is as follows:

$$\Delta U_s/EahL = b_1 W_o^2 + b_2 W_o^4 + b_3 W_o^6 \qquad (12)$$

where

$b_1 = f_1 + K_6 r^2$,
$b_2 = f_2 - (K_7 - f_3) r^2 + K_1 r^4 - \varphi_1$,
$b_3 = f_4 + (K_8 - f_5) r^2 + (K_3 + f_6) r^4 - \varphi_2 - g$, and
$r = a/L$

The f_i's, φ_i's, and g_i's are functions of the ratio a/L and n, and the K_i's are functions of n only. Expressions defining these functions are given in the Appendix. ΔU due to bending stresses is as follows:

$$\Delta U_b/EahL = (h^2/a^2) W_o^2 (C_1 + C_2 W_o^2 + C_3 W_o^4) \qquad (13)$$

where

$$C_1 = \pi/[48(1 - \nu^2)] \left(n^2 + 2\pi^2 r^2 \{1 + [\nu/(n^2 - 1)]\} + [\pi^4 n^2 r^4/(n^2 - 1)^2]\right),$$

$$C_2 = \pi/[256(1 - \nu^2)] \left(n^2 + \pi^2 r^2 \{1 + [\nu/(n^2 - 1)]\} + \tfrac{2}{3}\pi^4 r^4 \{2 + [1/(4n^2 - 1)^2]\}\right), \text{ and}$$

$$C_3 = \pi/[12{,}288(1 - \nu^2)] \left(5n^2 + 2\pi^2 r^2 \{5 - 17\nu + [8\nu/(4n^2 - 1)]\}\right).$$

$\Delta\Omega_p$ due to external pressure is as follows:

$$\Delta\Omega_p/EahL = p/[E(h/a)^3] (h/a)^2 (-a_1 W_o^2 + a_2 W_o^4) \qquad (14)$$

where

$a_1 = \pi n^2/[4(n^2 - 1)]$, and

$a_2 = (3\pi/128)\left(1 - \{1/[2(4n^2 - 1)]\}\right)$.

Increment of Total Potential Energy

The increment of total potential energy, ΔV, which results from buckling, is given by

$$\Delta V = \Delta U_m + \Delta U_b + \Delta U_s + \Delta \Omega_p \tag{15}$$

Substituting Eqs. 12, 13, 8, and 14 in Eq. 15 yields ΔV for the case of all-around support as

$$\Delta V/EahL = (B_1 - \bar{A}a_1t^2)\, W_o^2 + (B_2 + \bar{A}a_2t^2)\, W_o^4 + B_3W_o^6 \tag{16}$$

where

$\bar{A} = p/[E(h/a)^3]$,
$\bar{D} = k_s a/[E(h/a)^3]$,
$t = h/a$,
$B_1 = b_1 + C_1t^2 + \bar{D}d_1t^2$,
$B_2 = b_2 + C_2t^2 + \bar{D}d_2t^2$, and
$B_3 = b_3 + C_3t^2$.

For the case of support on the outward acting lobes only, Eqs. 12, 13, 11, and 14 in Eq. 15 yield the same relation as Eq. 16 except that d_1 and d_2 are replaced by $\bar{d}_1$ and $\bar{d}_2$ as given in Eq. 11.

Euler and Energy Loads

According to Tsein's criterion, the increment of total potential energy from the unbuckled to the buckled configuration is equal to zero, that is,

$$\Delta V = 0 \tag{17}$$

Therefore, by setting Eq. 16 to zero, the expression for the critical pressure coefficient, $\bar{A} = p_{cr}/E(h/a)^3$, is

$$\bar{A} = (B_1 + B_2W_o^2 + B_3W_o^4)/(a_1t^2 + a_2t^2W_o^2) \tag{18}$$

Minimizing Eq. 18 with respect to W_o^2 gives

$$(a_2W_o^4/2a_1) - W_o^2 - \tfrac{1}{2}\,[(B_2/B_3) + (a_2B_1/a_1B_3)] = 0 \tag{19}$$

The smallest positive value of W_o^2 from Eq. 19 substituted in Eq. 18 gives the energy load. Note that the root W_o^2 of Eq. 19 must be positive. If the roots are either negative or imaginary, the energy load does not exist. In some cases, a positive root gives an energy load greater than the corresponding Euler load. For such cases, the energy load and Euler load merge, and the phenomenon of snap-through does not occur.

The Euler load can be obtained simply by setting $W_o^2 = 0$ in Eq. 18. Thus,

$$\bar{A}^{Euler} = B_1/a_1t^2 \tag{20}$$

METHOD OF SOLUTION

Uniform Surrounding Field

Equation 18 is solved by calculating the critical pressure for a given set of independent variables corresponding to several values of $\bar{A}$ (9). The minimum value is the true critical pressure. A computer code was written to obtain solutions for $\bar{A}$ for permutations of the length-to-radius ratio, L/a, thickness-to-radius ratio, h/a, and foundation

coefficient, $\bar{D}$. All calculations were based on a Poisson's ratio, ν, of 0.33. Plots of the computer output are shown in Figures 3 and 4.

Differences between the Euler load and the energy load (Figs. 3 and 4) are largest for small L/a, large a/h, and small $\bar{D}$. The difference is as large as 25 percent in some cases. The energy load approaches the Euler load as L/a increases, a/h decreases, and $\bar{D}$ increases. With short, thin cylinders, the Euler load at small values of $\bar{D}$ is nearly the same for both types of support considered. The same is true for the energy load. At large values of $\bar{D}$, type of support is much more important as is evident from the following considerations. For infinitely long cylinders, it can be shown that the Euler and the energy loads are identical and that for all-around support they may be expressed by the relation

$$\bar{A}^{EL} = \alpha + \beta\bar{D} \tag{21}$$

where

$\bar{A} = p_{cr}/[E(h/a)^3]$,
$\bar{D} = k_z a/[E(h/a)^3]$,
$\alpha = (n^2 - 1)/[12(1 - \nu^2)]$, and
$\beta = 1/(n^2 - 1)$.

The lower bound for the critical pressure is

$$\bar{A}^{EL} = 2\sqrt{\alpha\beta\bar{D}} = 0.6116\sqrt{\bar{D}} \qquad \text{for } \nu = 0.33 \tag{22}$$

Likewise, for infinitely long cylinders with lobar support (support only on the outward-deflecting lobes)

$$\bar{A}^{LO} = \alpha + 0.5\,\beta\bar{D} \tag{23}$$

The lower bound for lobar support is given by

$$\bar{A}^{LO} = \sqrt{2\alpha\beta\bar{D}} = 0.4325\sqrt{\bar{D}} \qquad \text{for } \nu = 0.33 \tag{24}$$

From the ratio of Eqs. 22 and 24, the influence of type of soil support is

$$p_{cr}^{EL}/p_{cr}^{LO} = \sqrt{2} \tag{25}$$

or about 40 percent difference.

The foundation coefficient, k_z, in Eq. 22 can be expressed in terms of the one-dimensional (confined) compression modulus by using the theory for soil-surrounded tubes (4). For concentrically surrounded tubes, the modulus of elastic support, $k_s = k_z a$, may be expressed in terms of the modulus of elasticity of the soil, E_s, by the relation plotted in Figure 5. Further, E_s is related to the confined compression modulus, M_s, by the expression

$$E_s = \tilde{C}M_s \tag{26}$$

where $\tilde{C} = [(1 + \nu_s)(1 - 2\nu_s)]/(1 - \nu_s)$.

From the theory of a soil-surrounded tube (4), it has been shown that the ratio of k_s to E_s is

$$\tilde{B} = k_s/E_s = [1 - (a/a_o)^2]/\{(1 + \nu_s)[1 + (a/a_o)^2(1 - 2\nu_s)]\} \tag{27}$$

where a and a_o are radii as shown in Figure 5.

It follows that

$$k_z a = \tilde{B}\tilde{C}M_s \tag{28}$$

Figure 1. System geometry.

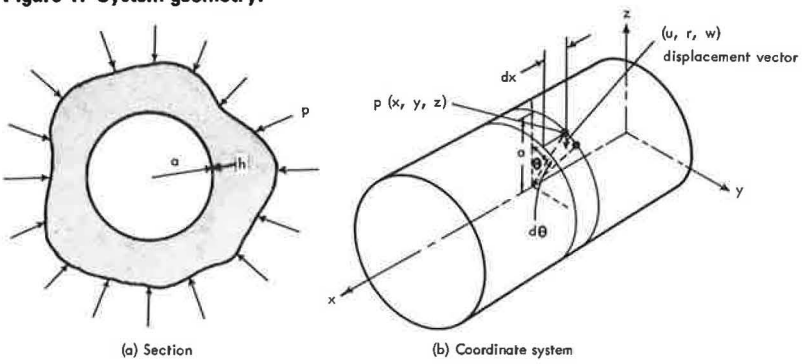

Figure 2. Pressure, energy, and displacement interrelations.

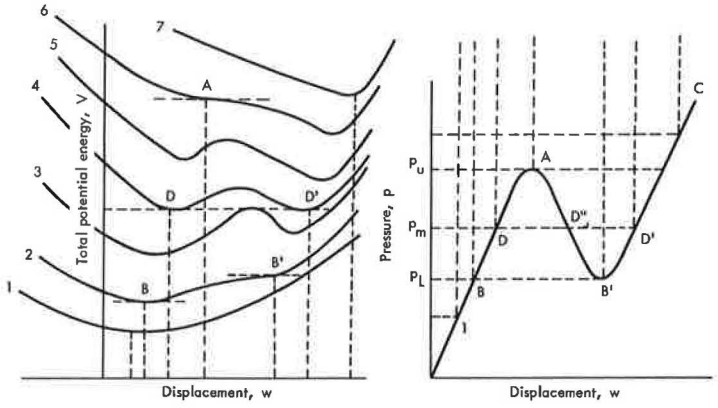

Figure 3. Variation of critical pressure with $\overline{D}$ for elastic support.

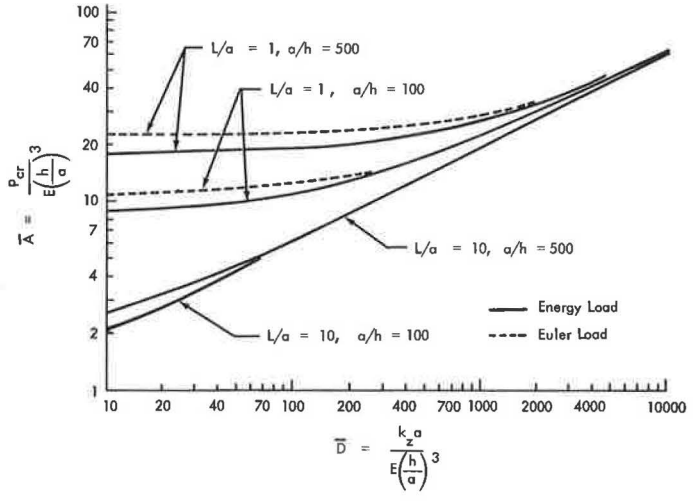

Figure 4. Variation of critical pressure with $\bar{D}$ for lobar support.

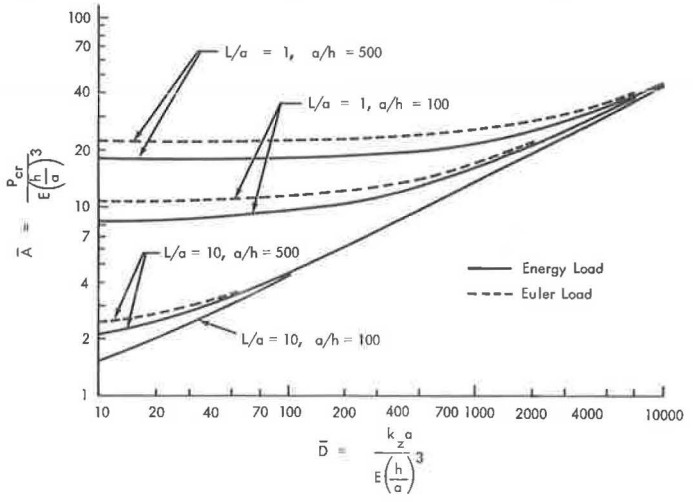

Figure 5. Modulus of soil support for elastic ring (4).

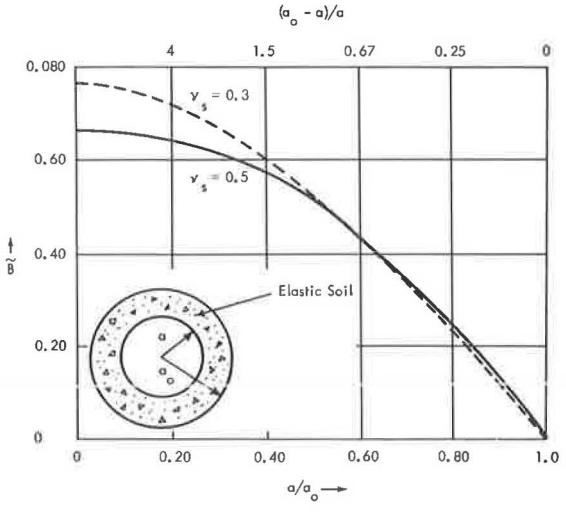

Figure 6. Buckling data.

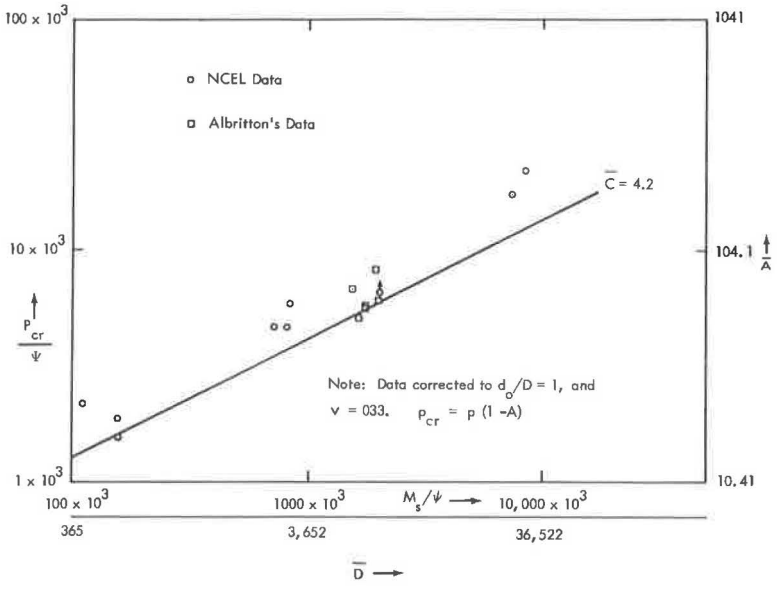

Substituting Eq. 27 in Eq. 22 gives

$$p_{cr}/\Psi = \overline{c}\sqrt{M_s/\Psi} \tag{29}$$

where

$\overline{c} = 6\sqrt{\widetilde{B}\widetilde{C}}$,
$\Psi = EI/D^3$,
D = mean diameter of cylinder, and
EI = stiffness of section.

In the strict mathematical sense, Eq. 29 is correct only for concentrically surrounded tubes. It is approximately correct, however, for cylinders buried beneath the earth's surface, which are loaded by the soil cover and possibly a uniform surface loading.

THEORY VERSUS EXPERIMENT

To facilitate a valid comparison of theory and experiment, we performed tests on thin metal cylinders in a segmented soil tank where the confined compression modulus, M_s, and the at-rest coefficient of lateral earth pressure, k, could be determined as an integral part of each test (10). All cylinders were 5 in. in diameter, 21 in. long, and either 6, 12, or 18 mils thick. Sand type and density were varied to get a wide range of confined compression moduli. A dry, rounded sand and a sharp-grained sand were used, each at three different densities. Measurements included surface pressure, cylinder deflections, and strains in the soil, tank, and cylinder. Details of the experiment may be found elsewhere (10).

The experimental data are plotted together with Eq. 29 in Figure 6. The buckling load was taken as $p_{cr} = p_f(1 - A)$ where p_f is the surface pressure at failure, and the arching was calculated from the corresponding strains at the haunches. The soil modulus used was the secant modulus at the failure load. All data plotted were corrected to one-diameter depth of cover.

Representative data from Albritton's tests (11) (SDA1, SDA2, SE1, SE2, SF1, and SF2) are also plotted in Figure 6. In these data, the moduli were from confined compression data. No other data are known to the authors in which all the necessary parameters are available. As may be seen, however, the Naval Civil Engineering Laboratory and the Albritton data agree reasonably well with the theory. There is, of course, the expected spread common to buckling and soil test data.

In general, the experimental buckling loads are greater than those from Eq. 29. This is considered to be due to greater compaction of the soil in the vicinity of the cylinder than at corresponding depths in the free-field. As a consequence, elastic support gives a better approximation of actual buckling loads than does lobar support.

Soil moduli back-calculated from deflections were in close agreement with measured values. This adds to confidence in the validity of the experimental data.

Predicting the surface and overburden pressure to cause buckling of a buried cylinder involves a determination of the arching over the structure (12). The percentage of the applied load that reaches the interface may vary by a factor of 20 or more depending on the relative stiffness of the inclusion and the confining soil.

CONCLUSIONS

The theoretical analysis and the comparison of the theory with test data substantiate the following conclusions:

1. The energy load and the Euler load are significantly different only for conditions (low length-to-radii ratios, low values of the foundation coefficient, and large radii-to-thickness ratios) that are not commonly encountered in practice. The theory agrees reasonably well with applicable experimental results.
2. The critical load with elastic support around the total perimeter is considered the best model of actual buried cylinders.
3. The buckling resistance of long buried cylinders is principally dependent on the bending flexibility, the secant value of the confined compression modulus, and Poisson's

ratio of the confining media as defined by Eq. 29. Arching is extremely important in governing the percentage of the applied load that reaches the interface.

4. The theory is considered adequate for obtaining conservative estimates of the elastic buckling load of buried cylinders.

REFERENCES

1. Von Karman, T., and Tsein, H. S. The Buckling of Spherical Shells by External Pressure. Jour. Aeronautical Sciences, Vol. 7, 1939, pp. 43-50.
2. Friedrichs, K. O. On the Minimum Buckling Load for Spherical Shells. California Institute of Technology, Theodore von Karman Anniversary Volume, 1941, pp. 258-272.
3. Link, H. Beitrag zum Knickproblem des elastich gebetten Kreisbogenträgers. Stahlbau, Vol. 23, No. 7, July 1963.
4. Luscher, U. Buckling of Soil-Surrounded Tubes. Jour. Soil Mechanics and Foundations Div., Proc. ASCE, Vol. 92, No. SM6, Proc. Paper 4990, Nov. 1966.
5. Langhaar, H. L., and Boresi, A. P. Snap-Through and Post-Buckling Behavior of Cylindrical Shells Under the Action of External Pressure. Eng. Exp. Sta., Univ. of Illinois, Urbana, Bull. 443, 1957.
6. Kirstein, A. F., and Wenk, E., Jr. Observations of Snap-Through Action in Thin Cylindrical Shells Under External Pressure. The David W. Taylor Model Basin, Washington, D. C., Rept. 1062, Nov. 1956.
7. Forrestal, M. J., and Herrmann, G. Buckling of a Long Cylindrical Shell Surrounded by an Elastic Medium. Presented at ASCE Struct. Eng. Conf., Preprint 108, Oct. 1964.
8. Gjelsvik, A., and Bodner, S. R. Non-Symmetrical Snap-Buckling of Spherical Caps. Jour. Eng. Mechanics Div., Proc. ASCE, Vol. 88, No. EM5, Oct. 1962.
9. Chelapati, C. V. Critical Pressures for Radially Supported Cylinders. U. S. Naval Civil Eng. Laboratory, Port Hueneme, Calif., Tech. Note N-773, Jan. 1966.
10. Allgood, J. R., Ciani, J. B., and Lew, T. K. Influence of Soil Modulus on the Behavior of Cylinders Buried in Sand. U. S. Naval Civil Eng. Laboratory, Port Hueneme, Calif., Tech. Rept. R-582, June 1968.
11. Albritton, G. E. Behavior of Flexible Cylinders Buried in Sand Under Static and Dynamic Loading. Waterways Exp. Sta., Vicksburg, Miss., Rept. 1-821, April 1968.
12. Allgood, J. R. Structures in Soil Under High Loads. Presented at the ASCE Structural Eng. Conf., Portland, Ore., April 6-10, 1970.

APPENDIX

EXPRESSIONS FOR VARIOUS TERMS IN THE THEORETICAL DEVELOPMENT

$$K_1 = \frac{3\pi^5}{256(1 - \nu^2)(n^2 - 1)^2}$$

$$K_2 = \frac{51\pi^5}{65536(1 - \nu^2)(4n^2 - 1)^2}$$

$$K_3 = \frac{\pi^5\left[\frac{5n^2}{(4n^2 - 1)^2} + \frac{7n^2 - 1}{4n^2 - 1} + 2n^2\right]}{256(1 - \nu^2)(n^2 - 1)^2}$$

$$K_4 = \frac{\pi^2(n^2 + 1)}{8(n^2 - 1)^2}$$

$$K_5 = \frac{\pi^2}{128}\left[2 + \frac{4n^2 + 1}{(4n^2 - 1)^2}\right]$$

$$K_6 = \frac{\pi^3}{8(1 + \nu)(n^2 - 1)^2}$$

$$K_7 = \frac{\pi^3}{32(1 + \nu)}\left[\frac{-n^2}{(4n^2 - 1)^2} + \frac{2n^2 - 1}{2(n^2 - 1)(4n^2 - 1)} + \frac{3n^2 - 4}{4(n^2 - 1)^2}\right]$$

$$K_8 = \frac{\pi^3}{512(1 + \nu)}\left[\frac{1}{(4n^2 - 1)^2} - \frac{2}{(4n^2 - 1)} + 2\right]$$

$$K_9 = \frac{\pi^3 n(8n^2 + 1)}{16(n^2 - 1)(4n^2 - 1)}$$

$$K_{10} = \frac{\pi(1 - \nu)n(8n^2 - 3)}{32(4n^2 - 1)}$$

$$K_{11} = \frac{(1 - \nu)\pi n}{2(n^2 - 1)}$$

$$K_{12} = \frac{\pi(1 - \nu)n^2(2n^2 + 1)}{4(n^2 - 1)(4n^2 - 1)}$$

$$K_{13} = \frac{\pi^3}{4(n^2 - 1)}$$

$$K_{18} = \frac{\pi^3}{8(4n^2 - 1)}$$

$$\xi = \frac{n}{2r}\sqrt{\frac{1 - \nu}{2}}$$

$$\alpha = \pi^2 + 4\xi^2$$

$$\beta = 9\pi^2 + 4\xi^2$$

$$\gamma = 4\pi^2 + 4\xi^2$$

$$\delta = \pi^2 + 36\xi^2$$

$$f_1 = \frac{-\pi K_{11}^2}{4(1 - \nu^2)\alpha}$$

$$f_2 = \frac{\pi K_{10} K_{11}}{2(1 - \nu^2)\alpha}$$

$$f_3 = \frac{-\pi K_9 K_{11}}{2(1 - \nu^2)\alpha}$$

$$f_4 = \frac{-\pi K_{10}^2}{4(1 - \nu^2)} \left[\frac{1}{\alpha} + \frac{1}{\beta}\right]$$

$$f_5 = \frac{\pi K_9 K_{10}}{2(1 - \nu^2)} \left[-\frac{1}{\alpha} + \frac{3}{\beta}\right]$$

$$f_6 = \frac{-\pi K_9^2}{4(1 - \nu^2)} \left[\frac{1}{\alpha} + \frac{9}{\beta}\right]$$

$$\varphi_1 = \frac{\pi(K_{12} + K_{13} r^2)^2}{16(1 - \nu^2)\alpha} + \frac{\pi^3 \tanh 2\xi}{16(1 - \nu^2)\xi} \left[\frac{\pi r^2}{2(n^2 - 1)} - \frac{K_{12} + K_{13} r^2}{\alpha}\right]^2$$

$$\varphi_2 = \frac{\pi^3 K_{18} r^2 \tanh 2\xi}{4(1 - \nu^2)\gamma\xi} \left[\frac{\pi r^2}{2(n^2 - 1)} - \frac{K_{12} + K_{13} r^2}{\alpha}\right]$$

$$g = \frac{\pi}{4(1 - \nu^2)} \left[\frac{(K_{14} r^2 + K_{15})^2}{\delta} + \frac{(3K_{14} r^2 - K_{15})^2}{9\alpha}\right]$$